Trapping an Oxidized and Protonated Intermediate of the [FeFe]-Hydrogenase Cofactor under Mildly Reducing Conditions

Moritz Senger[a]*, Jifu Duan[b], Mariia Pavliuk[a], Ulf-Peter Apfel[c,d], Michael Haumann[e], and Sven T. Stripp[f]*

a) Department of Chemistry, Physical Chemistry, Uppsala University, 75120 Uppsala, Sweden
b) Faculty of Biology and Biotechnology, Photobiotechnology, Ruhr-Universität Bochum, 44801 Bochum, Germany
c) Faculty of Chemistry and Biochemistry, Small Molecule Activation, Ruhr-Universität Bochum, 44801 Bochum, Germany
d) Fraunhofer UMSICHT, Electrosynthesis, 46047 Oberhausen, Germany
e) Department of Physics, Biophysics of Metalloenzymes, Freie Universität Berlin, 14195 Berlin, Germany
f) Department of Physics, Experimental Molecular Biophysics, Freie Universität Berlin, 14195 Berlin, Germany

*To whom correspondence should be addressed
moritz.senger@kemi.uu.se and sven.stripp@fu-berlin.de

ABSTRACT

The H-cluster is the catalytic cofactor of [FeFe]-hydrogenase, a metalloenzyme that catalyzes the production of hydrogen gas (H_2). The H-cluster carries two cyanide and three carbon monoxide ligands, making it an excellent target for IR spectroscopy. In previous work, we identified an oxidized and protonated H-cluster species, whose IR signature differs from the oxidized resting state (**Hox**) by a small but distinct shift to higher frequencies. This 'blue shift' was explained by a protonation at the [4Fe-4S] sub-complex of the H-cluster. The novel species, denoted **HoxH**, was preferentially accumulated at low pH and in the presence of the exogenous reductant sodium dithionite (NaDT). When **HoxH** was reacted with H_2, the hydride state (**Hhyd**) was formed, a key intermediate of [FeFe]-hydrogenase turnover. A recent publication revisited our protocol for the accumulation of **HoxH** in wild-type [FeFe]-hydrogenase, concluding that inhibition by NaDT decay products rather than cofactor protonation causes the spectroscopic 'blue shift'. Here, we demonstrate that **HoxH** formation does not require the presence of NaDT (or its decay products), but accumulates also with the milder reductants tris(2-carboxyethyl)phosphine, dithiothreitol, or ascorbic acid, in particular at low pH. Our data consistently suggest that **HoxH** is accumulated when deprotonation of the H-cluster is impaired, thereby preventing the regain of the oxidized resting state **Hox** in the catalytic cycle.

INTRODUCTION

Hydrogenases are gas-processing metalloenzymes that catalyze hydrogen turnover ($2H^+ + 2e^- \rightleftharpoons H_2$) in archaea, bacteria, and certain algae.[1] Among the three different classes, [FeFe]-hydrogenases show the highest turnover frequencies with an estimated proton reduction rate exceeding 20,000 H_2/s.[2–4] Notably, this reaction occurs close to the H_2/H^+ standard potential of -420 mV vs. SHE[5], making [FeFe]-hydrogenase the most efficient biological catalysts for H_2 turnover and inspiring bioinorganic model system.[6–8]

The active site cofactor of [FeFe]-hydrogenase is comprised of a [4Fe-4S] cluster ($[4Fe]_H$) covalently attached *via* a cysteine sidechain to a unique diiron site, $[2Fe]_H$. The latter is coordinated with two cyanide (CN^-), three carbon monoxide (CO), and an 'azadithiolate' ligand (ADT). Together, $[4Fe]_H$ and $[2Fe]_H$ are referred to as 'H-cluster' (Fig. 1). In the oxidized resting state, **Hox**, the iron ion distal to the $[4Fe]_H$ cluster (Fe_d) shows an apical vacancy.[9] Here, protons and H_2 may bind during catalytic turnover, a CO molecule may bind to form a reversibly inhibited state (**Hox-CO**)[10], and O_2 may interact in more deleterious reactions.[11]

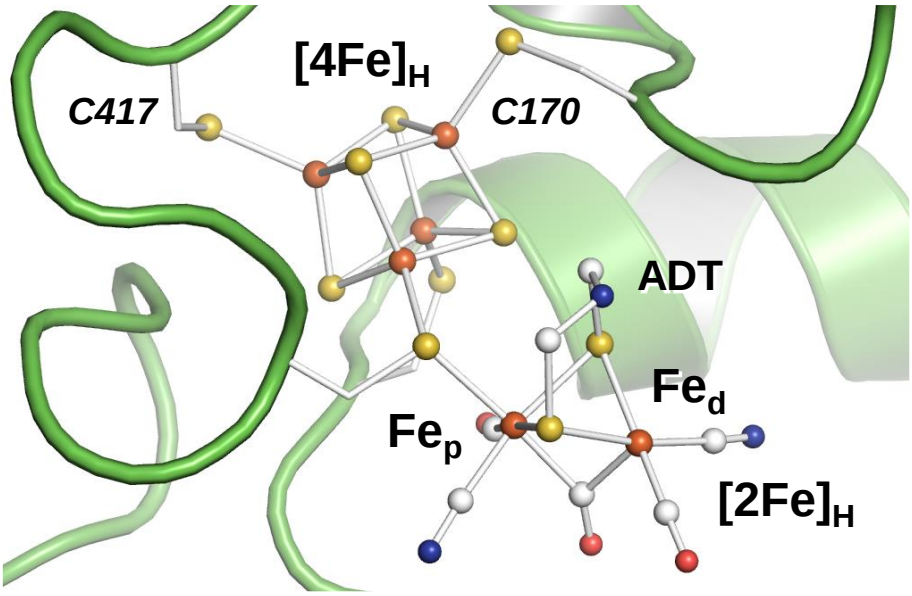

Figure 1. The catalytic cofactor of [FeFe]-hydrogenase. The distal iron ion of the $[2Fe]_H$ cluster (Fe_d) shows an apical vacancy where H_2 binds during catalytic turnover and protons are exchanged *via* the adt ligand (Fe_p, proximal iron ion). At the $[4Fe]_H$ cluster, cysteine C417 and/or C170 (*Cr*HydA1 numbering) may accept a proton in certain redox states. Drawn after PDB ID 4XDC.[12]

Both **Hox** and **Hox-CO** are defined by an oxidized [4Fe-4S] cluster ($[4Fe]_H^{2+}$) and a mixed-valence diiron site ($[Fe_p(II)Fe_d(I)]$).[13] Upon reduction of the [4Fe-4S] cluster ($[4Fe]_H^{1+}$), **Hred´** is formed. At variance with **Hox**, this state is diamagnetic and characterized by a small shift to lower frequencies of the CO/CN^- absorbance bands in the IR spectrum.[14] Reduction of the diiron site leads to **Hred**, which differs from **Hox** by a stronger effect on the IR signature, additionally complicated by changes in cofactor geometry at ambient temperature.[15] With respect to **Hred**, formation of the two-electron reduced state **Hsred** causes a small IR shift similar to the difference between **Hox** and **Hred´**.[16]

A key intermediate in the catalytic cycle is the so-called hydride state (**Hhyd**), characterized by a $[4Fe]_H^{1+}$, $[Fe_p(II)Fe_d(II)]$ configuration with an apical hydride ligand at Fe_d.[17–21] In previous work, we established a protocol to accumulate **Hhyd** in wild-type [FeFe]-hydrogenase. For this, the enzyme is exposed to acidic and reducing conditions, *i.e.*, pH 4 and 2 mM sodium dithionite ($Na_2S_2O_4$ or NaDT).[20] Before the reaction with H_2 favors accumulation of **Hhyd**, such samples adopt an oxidized species that differs from **Hox** by a distinct IR 'blue shift', *i.e.*, all cofactor bands shift to higher frequencies.[14] Moreover, the g_2 tensors of the rhombic EPR signal of **Hox** and **HoxH** are slightly different (2.044 and 2.048, respectively).[6] Both techniques exploit the diiron site to report on changes in the second coordination sphere of the H-cluster. Based on experimental and computational evidence, we found that protonation at a cysteine ligand of the $[4Fe]_H$ cluster (C417 and/or C170 in Fig. 1) accounts best for the 'blue shift', prompting us to suggest a novel H-cluster species, **HoxH**.[14] Similar protonation processes may occur in **Hred´** and **Hhyd**[22–24] although this view has been debated.[25]

Recently, Martini et al. revisited our protocol for the accumulation of **HoxH** in the [FeFe]-hydrogenase from *C. reinhardtii* (*Cr*HydA1).[26] The authors were concerned about the limited stability of NaDT in solution. Addition of Na_2SO_3 – a product of oxidative NaDT decay – indeed induced the 'blue shift' reaction, which led to the conclusion that **HoxH** represents a dithionite-inhibited species ('Hox-DT_i'). In the present study, we demonstrate that the formation of **HoxH** readily occurs in the presence of various mild reductants and does not require the presence of NaDT (or its decay products).

RESULTS AND DISCUSSION

*Cr*HydA1 was synthesized and activated as reported earlier.[27] The holoenzyme was carefully washed to remove any traces of NaDT (see Supporting Information for details). After concentration, the protein samples comprised ~1 mM *Cr*HydA1 in 10 mM Tris/HCl buffer (pH 8). To probe the **Hox** to **HoxH** transition with alternative reductants, we prepared solutions of 20 mM tris(2-carboxyethyl)phosphine (TCEP), dithiothreitol (DTT), or ascorbic acid in 200 mM 'mixed buffer' (PIPPS, MES, and Tris) adjusted to pH 4 (Fig. S1). The as-isolated protein sample was diluted 1:1 with 'mixed buffer' containing TCEP, DTT, ascorbic acid, or no reductant. The later samples were prepared at pH 4 or pH 8.

These five samples were characterized by *in situ* ATR FTIR spectroscopy under a stream of 'wet' N_2 aerosol or 'dry' N_2 gas (see Supporting Information for details on the preparation of protein films).[28] After 1–2 h incubation with N_2 in the preparatory stage of the experiment, all samples displayed a comparable composition of H-cluster states (~90% **Hox**, <10% **Hred**, and a very small fraction of **Hox-CO**, see Fig. S2). **Hred´** was exclusively observed in samples at pH 8, as acidic pH values suppress **Hred´** (Fig. S3).[16] While [FeFe]-hydrogenases prepared at pH 4 have been shown to adopt **HoxH** as main oxidized resting state in the presence of NaDT[20–22], we now found that **HoxH** is *not* observed at pH 4 when *Cr*HydA1 was mixed with TCEP, DTT, ascorbic acid, or no reductant (Fig. S2A).

The accumulation of **HoxH** is directly related to the pH value and the NaDT concentration but also affected by the presence of redox mediators and the protein concentration.[14,22] The latter observation was rationalized by intermolecular electron transfer in the densely packed sample film.[14] The protein concentration can be increased *in situ* by diminishing the water content in the sample film, switching from a 'wet' to a 'dry' N_2 gas stream – a unique feature of our ATR FTIR setup.[28] Fig. 2A depicts the global IR spectral changes upon partial dehydration of the *Cr*HydA1/TCEP protein film and the concomitant accumulation of **HoxH** over **Hox** in the frequency regime of the H-cluster (lower panel). Fig. 3A shows the respective changes in the time domain. Starting at time point t_0, the hydration level is tracked *via* the intensity of the symmetric OH stretching band of liquid water (ν_1) at 3360 cm^{-1}. The associated changes in protein concentration are followed *via* the amide II band of the protein backbone at 1540 cm^{-1}. The water content was decreased by up to 50% (*i.e.*, the ν_1 absorbance changes from ~0.45 to ~0.22). Sample

rehydration after time point t_2 led to a complete reversion of the observed changes. Fig. 2B shows how the initial increase of **Hox** between time points t_0 and t_1 (Δt = 2 min) is followed by a slower **Hox** to **HoxH** conversion. Afterwards, rehydration shifts the equilibrium immediately back to **Hox** without notable loss of cofactor integrity, highlighting the reversibility of the state conversion.

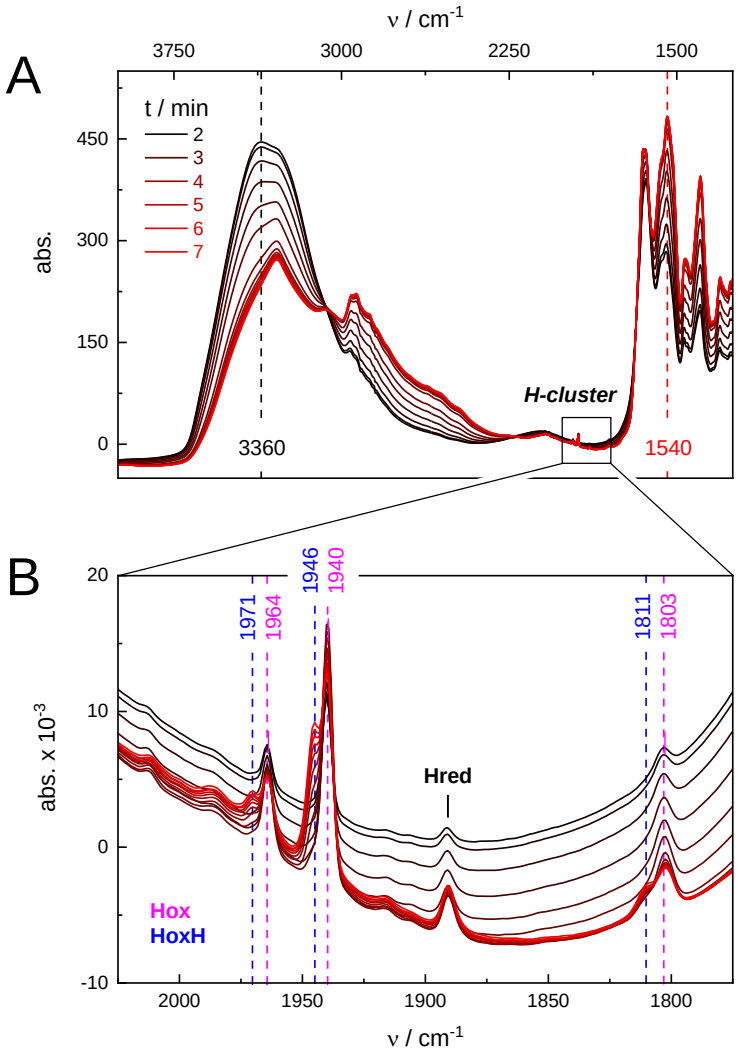

Figure 2. Accumulation of HoxH upon dehydration. ATR FTIR spectra of a *Cr*HydA1 protein film at pH 4 with 10 mM TCEP. **(A)** From black to red, the spectral changes upon dehydration of the protein film are shown. Bands at 3360 cm^{-1} and 1540 cm^{-1} are assigned to liquid water (ν_1) and protein (amide II), respectively. **(B)** The band changes in the CO frequency regime of the H-cluster are assigned to **Hox** and **HoxH** (magenta and blue labels, respectively). A residual fraction of **Hred** remains.

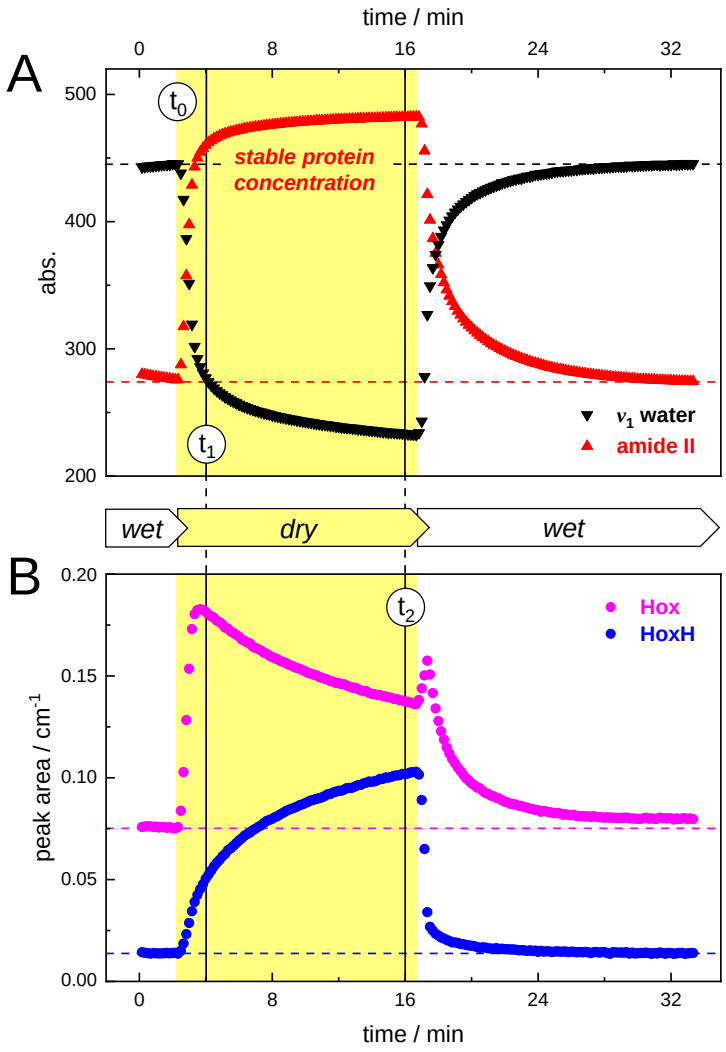

Figure 3. Kinetic evaluation of ATR FTIR data. (A) Plotting the ν_1 and amide II band intensity over time highlights the changes in hydration and protein concentration when the 'wet' N_2 aerosol is switched to 'dry' N_2 gas at t_0 (upper panel). Between t_1 and t_2, a relatively stable protein concentration is established before the system is switched back to 'wet' conditions. **(B)** Both **Hox** and **HoxH** increase with the protein concentration in the initial dehydration period between t_0 and t_1 while **Hox** slowly converts to **HoxH** in the dehydrated protein film. Note the reversibility of the **Hox** to **HoxH** transition upon rehydration of the protein film.

HoxH increases already between time points t_0 and t_1; however, the rapid increase of protein concentration after t_0 affects the **Hox** population more visibly as it represents the main H-cluster state at the beginning of the experiment. Between time points t_1 and t_2 (Δt = 12 min) the protein concentration was about constant (Fig. 3A), which facilitated a quantitative evaluation of the

CO/CN^- band shifts of the H-cluster *via* IR difference spectra (Fig. 3B). Within the spectral resolution of our experiment, all band positions are identical to those of **HoxH** as formed in the presence of NaDT (Fig. S4 and Tab. S1).[14] However, while near-complete state conversion was observed with 10 mM NaDT (>90%) in earlier experiments, the **HoxH** yield was only 50% when 10 mM TCEP was used. As discussed Supporting Information, this is presumably due to the ~250 mV less reducing redox potential of TCEP at pH 4 vs. NaDT. Following the dehydration protocol described above, the **Hox** to **HoxH** conversion was probed with samples containing 10 mM DTT or 10 mM ascorbic acid, resulting in 35% or 20% enrichment of **HoxH**, respectively (Fig. 4). In samples without reductant, only negligible **HoxH** was detected (Fig. S3). These results clearly emphasize the need for a reductant in **HoxH** formation and prove that NaDT is not required.

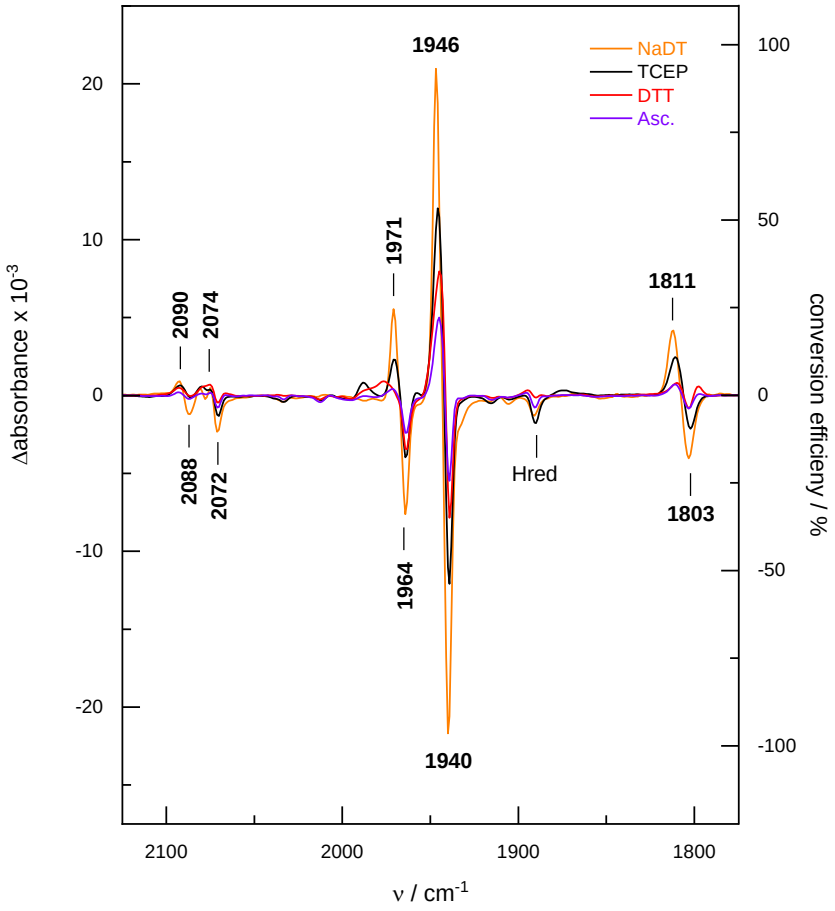

Figure 4. ATR FTIR difference spectra. Accumulation of **HoxH** (positive bands) over **Hox** (negative bands) over a time span of 12 min in partially dehydrated *Cr*HydA1 protein films at pH 4 and in the presence of reductants TCEP (black), DTT (red), or ascorbic acid (violet). For reference, the >90% conversion of **Hox** into **HoxH** in the presence of NaDT is shown (orange) that defines the conversion efficiency (right X-axis).

Although direct experimental proof for a protonated cysteine ligand is yet to obtain, the present findings reinforce our model for the accumulation of **HoxH** *via* a transiently reduced and protonated $[4Fe]_H$ cluster (Fig. S5).[14,22] After oxidation of the H-cluster due to proton reduction and H_2 release, acidic conditions stabilize **HoxH** (proton 'backpressure') whereas **Hox** is regained under alkaline conditions. This model is supported by the low but significant H_2 release activity of *Cr*HydA1 in the presence of TCEP, DTT, or ascorbic acid (Fig. S6). Protonation of the $[4Fe]_H$ cluster may advance *via* a regulatory proton pathway that is conserved among standard [FeFe]-hydrogenases[14] and differs from the catalytic proton pathway to the diiron site.[29,30] This proton is therefore not part of the hydrogen turnover reaction but may impede a premature reduction and protonation of the diiron site.[31]

CONCLUSIONS

In summary, we demonstrated that **HoxH** formation does not require NaDT (or its decay products) but can be induced in the presence of mild reductants like TCEP, DTT, or ascorbic acid. The suggested nomenclature 'Hox-DT_i' is inadequate.[26] The accumulation of **HoxH** upon partial dehydration might be related to intermolecular electron transfer, the increase of reductant concentration, and a relative decrease in pH in the film.[14] We speculate that solvent access to the H-cluster is hampered in the dehydrated protein film so that proton release from the $[4Fe]_H$ cluster is slowed down or even impaired. This effect then leads to accumulation of **HoxH** in the presence of mild reductants that drive the catalytic cycle at a lower rate than NaDT. Since protein film electrochemistry hinted at an inhibitory effect of Na_2SO_3 on *Cr*HydA1[26], we will join Martini et al. in emphasizing that potentially 'non-innocent' reductants like NaDT should be used with great care in hydrogenase preparations and activity essays. The accumulation of a protonated [4Fe-4S] cluster under mildly reducing conditions now suggests that proton-coupled electron transfer involving a cysteine ligand may represent a general redox tuning mechanism.[31] Similar concepts have been employed to explain the redox chemistry of ferredoxins, Rieske proteins, mitoNEET, and other metalloproteins.[32–35]

ACKNOWLEDGMENTS

The European Union's Horizon 2020 research and innovation program is gratefully acknowledged for funding to MS (Marie Skłodowska-Curie Grant No. 897555). JD is grateful for funding by the DFG (project no. 461338801). UPA acknowledges funding by the DFG (under Germanys' Excellence Strategy – EXC 2033–390677874) and the Fraunhofer Internal Programs (Grant No. ATTRACT 097- 602175). MH thanks UniSysCat (Cluster of Excellence Berlin) for financial support. STS is funded by the DFG within the framework of SPP 1927 priority program 'Iron-Sulfur for Life' (Grant No. STR1554/5-1). We thank Petko Chernev (Universitet Uppsala, Sweden) for providing the IR curve fitting software 'GloGaussFit'.

REFERENCES

[1] W. Lubitz, H. Ogata, O. Rüdiger, E. Reijerse, *Chem. Rev.* **2014**, *114*, 4081–4148.

[2] V. Fourmond, E. S. Wiedner, W. J. Shaw, C. Léger, *J. Am. Chem. Soc.* **2019**, *141*, 11269–11285.

[3] V. Fourmond, N. Plumeré, C. Léger, *Nat. Rev. Chem.* **2021**, *5*, 348–360.

[4] C. Madden, M. D. Vaughn, I. Díez-Pérez, K. A. Brown, P. W. King, D. Gust, A. L. Moore, T. A. Moore, *J. Am. Chem. Soc.* **2012**, *134*, 1577–1582.

[5] G. Goldet, C. Brandmayr, S. T. Stripp, T. Happe, C. Cavazza, J. C. Fontecilla-Camps, F. A. Armstrong, *J. Am. Chem. Soc.* **2009**, *131*, 14979–14989.

[6] H. Land, M. Senger, G. Berggren, S. T. Stripp, *ACS Catal.* **2020**, *10*, 7069–7086.

[7] J. T. Kleinhaus, F. Wittkamp, S. Yadav, D. Siegmund, U. P. Apfel, *Chem. Soc. Rev.* **2021**, *50*, 1668–1784.

[8] J. A. Birrell, P. Rodríguez-Maciá, E. J. Reijerse, M. A. Martini, W. Lubitz, *Coord. Chem. Rev.* **2021**, *449*, 214191.

[9] Y. Nicolet, C. Piras, P. Legrand, C. E. Hatchikian, J. C. Fontecilla-Camps, *Structure* **1999**, *7*, 13–23.

[10] M. Senger, S. Mebs, J. Duan, F. Wittkamp, U.-P. Apfel, J. Heberle, M. Haumann, S. T. Stripp, *Proc. Natl. Acad. Sci. U. S. A.* **2016**, *113*, 8454–8459.

[11] J. Esselborn, L. Kertess, U.-P. Apfel, E. Hofmann, T. Happe, *J. Am. Chem. Soc.* **2019**, *141*, 17721–17728.

[12] J. Esselborn, N. Muraki, K. Klein, V. Engelbrecht, N. Metzler-Nolte, U.-P. Apfel, E.

Hofmann, G. Kurisu, T. Happe, *Chem. Sci.* **2016**, *7*, 959–968.

[13] W. Lubitz, E. Reijerse, M. van Gastel, *Chem. Rev.* **2007**, *107*, 4331–4365.

[14] M. Senger, S. Mebs, J. Duan, O. Shulenina, K. Laun, L. Kertess, F. Wittkamp, U.-P. Apfel, T. Happe, M. Winkler, M. Haumann, S. T. Stripp, *Phys. Chem. Chem. Phys.* **2018**, *20*, 3128–3140.

[15] S. T. Stripp, S. Mebs, M. Haumann, *Inorg. Chem.* **2020**, *59*, 16474–16488.

[16] K. Laun, I. Baranova, J. Duan, L. Kertess, F. Wittkamp, U.-P. Apfel, T. Happe, M. Senger, S. T. Stripp, *Dalt. Trans.* **2021**, *50*, 3641–3650.

[17] D. W. Mulder, M. W. Ratzloff, M. Bruschi, C. Greco, E. Koonce, J. W. Peters, P. W. King, *J. Am. Chem. Soc.* **2014**, *136*, 15394–15402.

[18] D. W. Mulder, Y. Guo, M. W. Ratzloff, P. W. King, *J. Am. Chem. Soc.* **2017**, *139*, 83–86.

[19] E. J. Reijerse, C. C. Pham, V. Pelmenschikov, R. Gilbert-Wilson, A. Adamska-Venkatesh, J. F. Siebel, L. B. Gee, Y. Yoda, K. Tamasaku, W. Lubitz, T. B. Rauchfuss, S. P. Cramer, *J. Am. Chem. Soc.* **2017**, *139*, 4306–4309.

[20] M. Winkler, M. Senger, J. Duan, J. Esselborn, F. Wittkamp, E. Hofmann, U.-P. Apfel, S. T. Stripp, T. Happe, *Nat. Commun.* **2017**, *8*, 16115.

[21] V. Pelmenschikov, J. A. Birrell, C. C. Pham, N. Mishra, H. Wang, C. Sommer, E. Reijerse, C. P. Richers, K. Tamasaku, Y. Yoda, T. B. Rauchfuss, W. Lubitz, S. P. Cramer, *J. Am. Chem. Soc.* **2017**, *139*, 16894–16902.

[22] M. Senger, K. Laun, F. Wittkamp, J. Duan, M. Haumann, T. Happe, M. Winkler, U.-P. Apfel, S. T. Stripp, *Angew. Chemie Int. Ed.* **2017**, *56*, 16503–16506.

[23] S. Mebs, J. Duan, F. Wittkamp, S. T. Stripp, T. Happe, U.-P. Apfel, M. Winkler, M. Haumann, *Inorg. Chem.* **2019**, *58*, 4000–4013.

[24] J. Duan, S. Mebs, K. Laun, F. Wittkamp, J. Heberle, E. Hofmann, U.-P. Apfel, M. Winkler, M. Senger, M. Haumann, S. T. Stripp, *ACS Catal.* **2019**, *9*, 9140–9149.

[25] P. Rodríguez-Maciá, N. Breuer, S. DeBeer, J. A. Birrell, *ACS Catal.* **2020**, *10*, 13084–13095.

[26] M. A. Martini, O. Rüdiger, N. Breuer, B. Nöring, S. DeBeer, P. Rodríguez-Maciá, J. A. Birrell, *J. Am. Chem. Soc.* **2021**, *143*, 18159–18171.

[27] J. Esselborn, C. Lambertz, A. Adamska-Venkatesh, T. Simmons, G. Berggren, J. Noth, J. Siebel, A. Hemschemeier, V. Artero, E. Reijerse, M. Fontecave, W. Lubitz, T. Happe, *Nat. Chem. Biol.* **2013**, *9*, 607–609.

[28] S. T. Stripp, *ACS Catal.* **2021**, *11*, 7845–7862.

[29] J. Duan, M. Senger, J. Esselborn, V. Engelbrecht, F. Wittkamp, U.-P. Apfel, E. Hofmann, S. T. Stripp, T. Happe, M. Winkler, *Nat. Commun.* **2018**, *9*, 4726.

[30] M. Senger, V. Eichmann, K. Laun, J. Duan, F. Wittkamp, G. Knör, U.-P. Apfel, T. Happe, M. Winkler, J. Heberle, S. T. Stripp, *J. Am. Chem. Soc.* **2019**, *141*, 17394–17403.

[31] M. Haumann, S. T. Stripp, *Acc. Chem. Res.* **2018**, *51*, 1755–1763.

[32] K. Chen, C. A. Bonagura, G. J. Tilley, J. P. McEvoy, Y.-S. Jung, F. A. Armstrong, C. D. Stout, B. K. Burgess, *Nat. Struct. Biol.* **2002**, *9*, 188–192.

[33] Y. Zu, M. M. J. Couture, D. R. J. Kolling, A. R. Crofts, L. D. Eltis, J. A. Fee, J. Hirst, *Biochemistry* **2003**, *42*, 12400–12408.

[34] J. A. Zuris, D. A. Halim, A. R. Conlan, E. C. Abresch, R. Nechushtai, M. L. Paddock, P. A. Jennings, *J. Am. Chem. Soc.* **2010**, *132*, 13120–13122.

[35] J. Liu, S. Chakraborty, P. Hosseinzadeh, Y. Yu, S. Tian, I. Petrik, A. Bhagi, Y. Lu, *Chem. Rev.* **2014**, *114*, 4366–4369.

Supporting Information

Contents

Preparation of *Cr*HydA1 holoenzyme. *Cr*HydA1 apo-protein with a *C*-terminally fused strep-tagII was expressed and synthesized in *E. coli* strain BL21(DE3) ΔiscR under anaerobic conditions as described by Kuchenreuther and co-workers.[1] At variance with this protocol, the [FeFe]-hydrogenase-specific maturases HydEFG were not co-expressed, resulting in the production of inactive *Cr*HydA1 apo-protein.[2] Protein purification was achieved by strep-tactin affinity chromatography under strictly anaerobic conditions with a 10 mM Tris-HCl buffer (pH 8.0) and 2 mM NaDT as described by von Abendroth and co-workers.[3]

The ADT complex $[FeFe[m\text{-}(SCH_2)_2NH](CN)_2(CO)_4][Et_4N]_2$ was synthesized and purified as described by Li and Rauchfuss.[4] Maturation of *Cr*HydA1 apo-protein with a tenfold excess of the ADT complex was achieved by incubation for ~1 h at 24 °C in 100 mM potassium phosphate buffer (pH 6.8) with 2 mM NaDT to ensure reducing conditions as described by Esselborn and co-workers.[5] The activated *Cr*HydA1 holoenzyme was subsequently cleaned from residual ADT complex and NaDT by use of a NAP™ 5 (GE Healthcare) size exclusion chromatography and adjusted to pH 8 in 10 mM Tris-HCl buffer. In the absence of H_2, no reduction of methyl viologen was observed, and no traces of **HoxH** were observed when the sample was adjusted to pH 4. These data prove that the samples are completely NaDT-free. Enzyme preparations were concentrated to ~1 mM *Cr*HydA1 (~48 g/L) using Amicon Ultra centrifugal filters 30 K (Millipore) and stored at -80 °C under strictly anaerobic conditions.

***In situ* ATR FTIR spectroscopy.** The FTIR spectrometer (Tensor27, Bruker Optik, Germany) was equipped with a triple-reflection ZnSe/Si crystal ATR cell (Smith Detection, USA) and placed in an anaerobic chamber (Coy Laboratories, USA). Infrared spectra were recorded with 80 kHz scanning velocity at a spectral resolution of 2 cm^{-1}. Under these conditions, the time-resolution of data acquisition is in the range of 1 s (one interferometer scan in the forward/backward direction).

To prepare a protein film, 1 µL *Cr*HydA1 solution (~1 mM) was pipetted onto the silicon crystal of the ATR cell and enclosed by a custom-made gas titration cell[6] to concentrate the sample under a stream of dry N_2 gas. Once ~60% of water was removed from the protein solution, a relatively dry protein film was formed. Then, the gas was sent through a reservoir of 150 mL aqueous buffer, creating a 'wet' aerosol that was used to rehydrate the hygroscopic protein film. Changing between dry gas and wet aerosol, the humidity of the protein film can be controlled. Further details of the experimental setup can be found in reference [6].

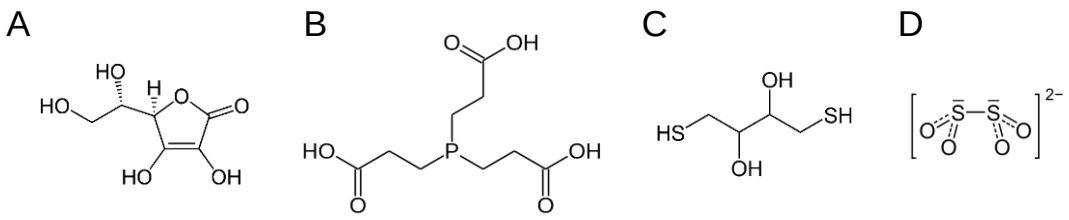

Figure S1. Reductants discussed in this study. (A) Ascorbic acid ('Vitamin C', E^0 = -80 mV vs. SHE). **(B)** Tris(2-carboxyethyl)phosphine (TCEP, E^0 = -290 mV vs. SHE). **(C)** Dithiothreitol (DTT, E^0 = -330 mV vs. SHE). Based on literature reports, a redox potential of -240 mV, -200 mV, or -160 mV for DTT, TCEP, or ascorbic acid is assumed at pH 4.[7–9] **(D)** Sodium dithionite ($Na_2S_2O_4$) has a standard potential of E^0 = -660 mV vs. SHE (approximately -450 mV at pH 4).[10]

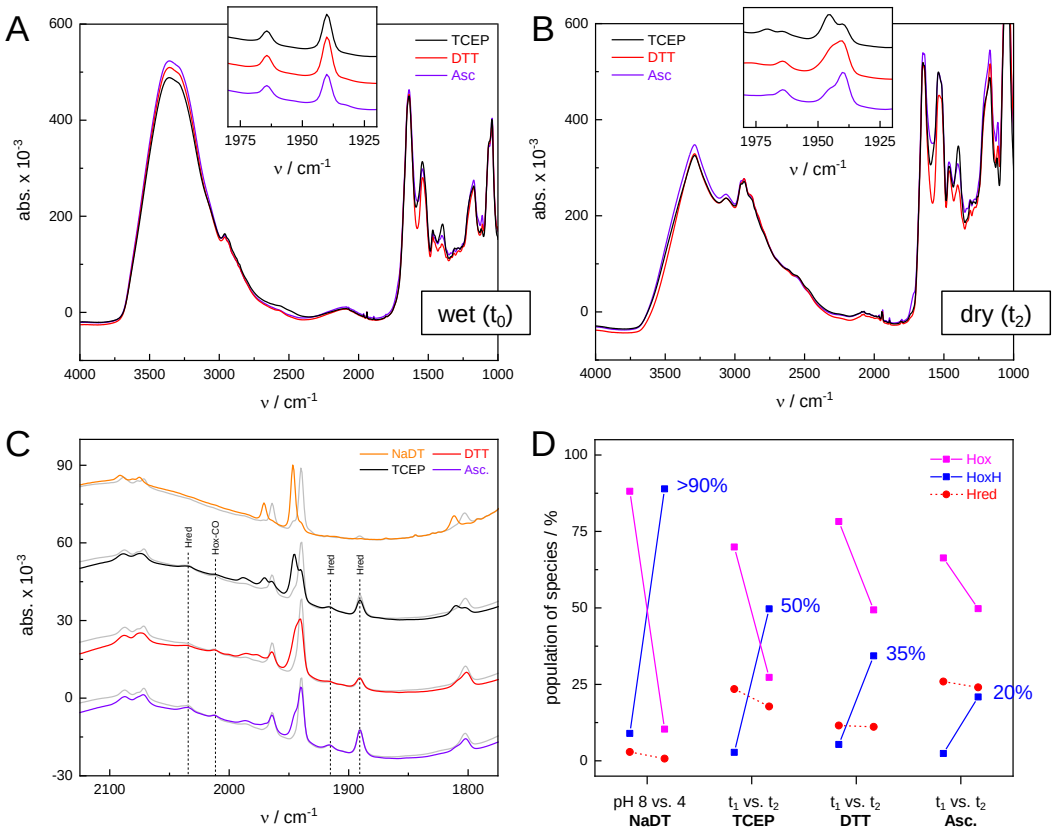

Figure S2. ATR FTIR absorbance spectra. Absorbance spectra of **(A)** fully hydrated ('wet' = t_0) and **(B)** partially dehydrated protein films ('dry' = t_2) of *Cr*HydA1 samples with 10 mM TCEP, DTT, or ascorbic acid at pH 4. The 'dry' film contains ~50% liquid water relative to fully hydrated conditions, based on the intensity of the OH band of liquid water at 3360 cm^{-1} as plotted in Figure 2B of the main text. The inset in panel (A) and (B) shows a representative section of the CO-vibrational frequency range of the H-cluster, highlighting the changes in the **Hox** and **HoxH** populations. Upon dehydration, which causes an increase of the protein and reductant concentration in the film and may decrease the pH[11], **HoxH** is accumulated at the expense of **Hox**. Spectra in (A) were recorded after 1–2 h under a 'wet' N_2 aerosol. Note the lack of **HoxH** under these conditions. **(C)** Full CO/CN^- frequency regime of the H-cluster, comparing the spectra at t_1 (grey traces) and t_2 (colored traces) for different reductants. Sample dehydration was started at t_0, resulting in larger changes in protein concentration (see Figure 2B in the main text). Between time points t_1 and t_2, however, the protein concentration was about constant, so these spectra were used to calculate the difference spectra of Figure 3 in the main text. Residual H-cluster species in the **Hred** and **Hox-CO** state are annotated. For comparison, spectra in the presence of 10 mM NaDT at pH 8 (grey) and pH 4 (orange) are shown.[11] **(D)** Quantitative evaluation of the state populations for **Hox**, **HoxH**, and **Hred** at t_1 and t_2 (time points as defined in Figure 2B in the main text). All reductants facilitate significant **Hox** to **HoxH** conversion, with TCEP and DTT being more effective (50% and 35% **HoxH**) than ascorbic acid (20% **HoxH**). In the presence of NaDT, more than 90% **HoxH** is accumulated when switched from pH 8 to pH 4 *in situ*.[11]

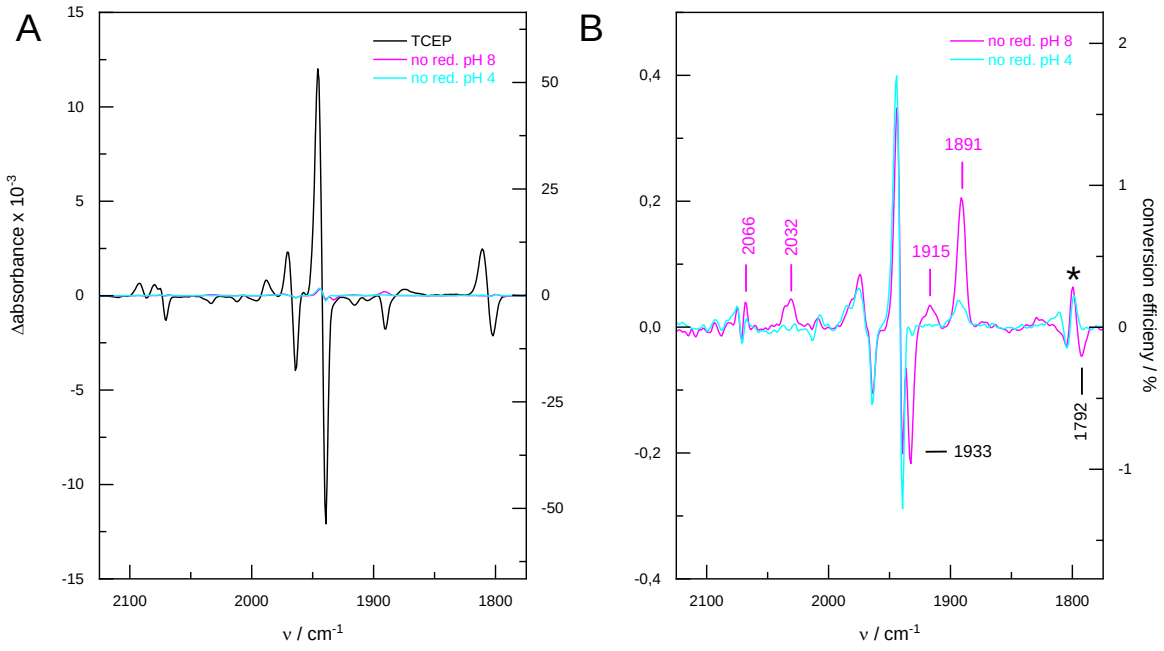

Figure S3. Reference ATR FTIR difference spectra. (A) When reductants were completely absent in *Cr*HydA1 preparations at pH 8 or pH 4, less than 2% **Hox** to **HoxH** conversion was observed upon partial dehydration (compare conversion efficiency axis in (B)). The difference spectrum of the sample with TCEP is plotted for comparison. **(B)** A close-up reveals a band at 1800 cm^{-1} (*), which presumably is due to a small population of **Hred´H** at both pH values.[12] Moreover, the pH 8 sample shows a conversion of **Hred´** (bands at 1933 and 1792 cm^{-1}) to **Hred** (bands at 2066, 2032, 1915, and 1891 cm^{-1}) that is not observed in any pH 4 preparation. This is expected because acidic conditions suppress **Hred´** and favor accumulation of **Hred** and **Hsred**.[13]

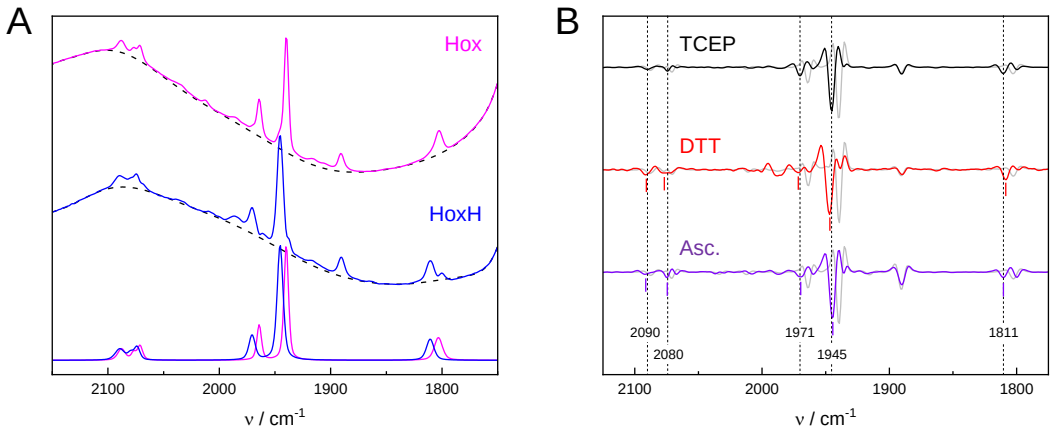

Figure S4. Evaluation of the spectral signatures of Hox and HoxH. (A) Partial subtraction of the FTIR absorbance spectra of the sample with TCEP at t_1 and t_2 (see Figure 2 in the main text) facilitated the generation of practically pure spectra for **Hox** (magenta) and **HoxH** (blue). Raw spectra were fitted with a polynomial baseline (dashed traces) and five Voigt profiles of defined frequency, full-width-at-half-maximum (fwhm), and intensity ratio (see Table S1). In-house software was used for the fitting procedure, as reported earlier.[11] The fitted spectra are shown at the bottom of panel (A). **(B)** Second derivative analysis of the pure spectra of **Hox** and **HoxH** as observed in the presence of TCEP, DTT, or ascorbic acid supports the IR band positions as suggested by the fit results (Table S1). The small **HoxH** band shifts are in the range of the spectral resolution of the experiment (2 cm^{-1}, see Supporting Methods).

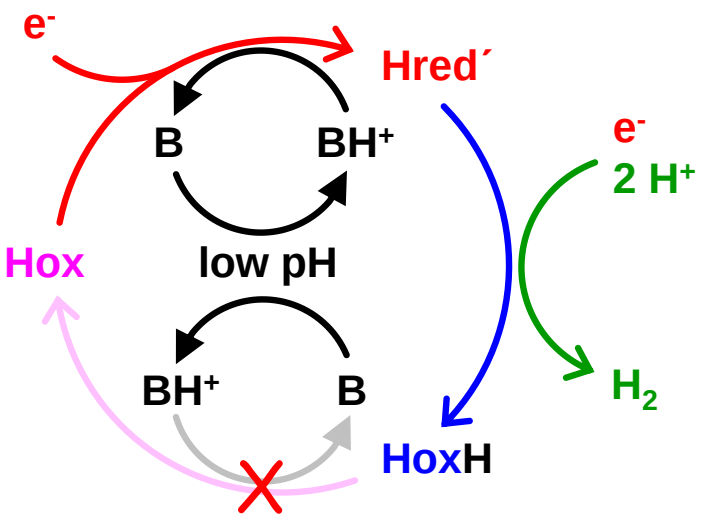

Figure S5. Accumulation of HoxH. The oxidized state **Hox** is converted into a state resembling **Hred´** by one-electron reduction of the [4Fe-4S] cluster and protonation of a cysteine ligand *via* an adjacent base (B, presumably a water molecule).[11–13] Reducing equivalents (e^-) may stem from NaDT, TCEP, DTT, or ascorbic acid. In a second PCET step, a proton is reduced to a terminal hydride ligand at Fe_d of the diiron site (resembling **Hhyd**, not shown in the scheme), which reacts with another proton to form H_2 gas. At high pH, **Hox** is recovered *via* deprotonation of the [4Fe-4S] cluster and re-protonation of the adjacent base. The scheme depicts the situation at low pH. Here, **HoxH** accumulates when the base is protonated (BH^+) and regain of **Hox** is impaired.

Table S1. Fit parameters of ATR FTIR spectra.

state	ν / cm^{-1}	fwhm / cm^{-1}	rel. amplitude
Hox	1803.2	8.6	0.35
Hox	1939.9	4.8	1.00
Hox	1964.2	4.9	0.31
Hox	2071.2	5.5	0.14
Hox	2087.9	8.0	0.16
HoxH	1810.6	8.0	0.23
HoxH	1945.4	6.3	1.00
HoxH	1970.6	6.7	0.23
HoxH	2079.6	6.0	0.05
HoxH	2089.4	10.0	0.15

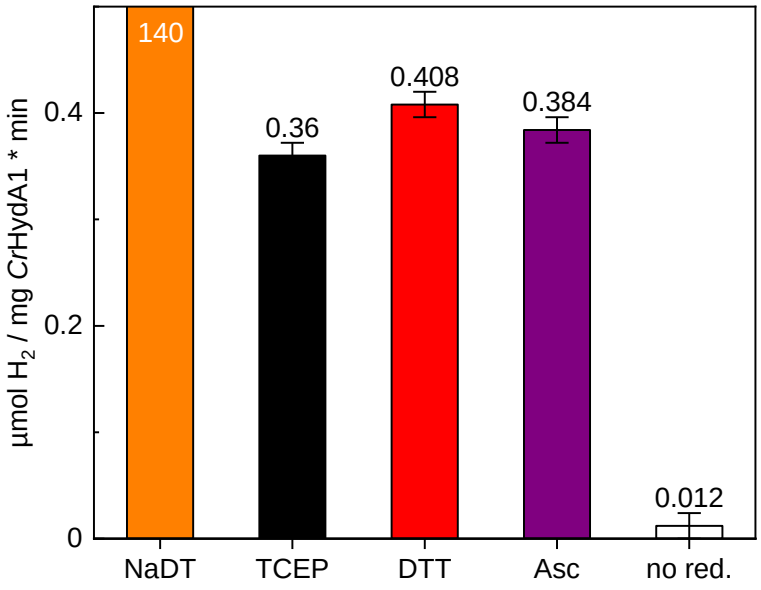

Figure S6. Activity measurements. *In vitro* H_2 release activity was determined for various reductants. Specifically, 35 nmol *Cr*HydA1 was mixed with phosphate buffer (100 mM, pH 7) inside the glovebox with humid Ar atmosphere (total reaction volume 800 µL). Then hydrogenase samples in buffer were loaded to 37 °C water bath for 10 min. Meanwhile, reductants were purged with argon for 20 min. After incubation of hydrogenase samples in the bath, 100 µL of 890 mM reductant stock solution was injected with the Hamiltonian syringe (resulting in ~100 mM NaDT, TCEP, DTT, or ascorbic acid). A reference sample was prepared with no reductant at all. Samples with *Cr*HydA1 and reductants were incubated in a 37 °C water bath for another 15 min. Finally, 100 µL of the gas phase (total headspace volume ~8.1 mL) was analyzed for H_2 by gas chromatography as reported earlier.[3] We detected 3500, 9.0, 10.2, 9.6, and 0.3 nmol H_2, which was calculated into specific activity (µmol H_2 / mg *Cr*HydA1 x min) as plotted above. To meet the conditions in the FTIR experiment, methyl viologen (MV) was not used in the activity assays, which explains why the H_2 release activity with NaDT is less than10% of the values reported for activity assays with MV.[5]

Supporting References

[1] J. M. Kuchenreuther, C. S. Grady-Smith, A. S. Bingham, S. J. George, S. P. Cramer, J. R. Swartz, *PLoS One* **2010**, *5*, e15491.

[2] D. W. Mulder, D. O. Ortillo, D. J. Gardenghi, A. V. Naumov, S. S. Ruebush, R. K. Szilagyi, B. Huynh, J. B. Broderick, J. W. Peters, *Biochemistry* **2009**, *48*, 6240–6248.

[3] G. von Abendroth, S. T. Stripp, A. Silakov, C. Croux, P. Soucaille, L. Girbal, T. Happe, *Int. J. Hydrogen Energy* **2008**, *33*, 6076–6081.

[4] H. Li, T. B. Rauchfuss, *J. Am. Chem. Soc.* **2002**, *124*, 726–727.

[5] J. Esselborn, C. Lambertz, A. Adamska-Venkatesh, T. Simmons, G. Berggren, J. Noth, J. Siebel, A. Hemschemeier, V. Artero, E. Reijerse, M. Fontecave, W. Lubitz, T. Happe, *Nat. Chem. Biol.* **2013**, *9*, 607–609.

[6] S. T. Stripp, *ACS Catal.* **2021**, *11*, 7845–7862.

[7] I. B. Santarino, S. C. B. Oliveira, A. M. Oliveira-Brett, *Electrochem. commun.* **2012**, *23*, 114–117.

[8] L. Peng, X. Xu, M. Guo, X. Yan, S. Wang, S. Gao, S. Zhu, *Metallomics* **2013**, *5*, 920–927.

[9] H. Borsook, G. Keighley, *Proc. Natl. Acad. Sci.* **1933**, *19*, 875–878.

[10] S. G. Mayhew, *Eur. J. Biochem.* **1978**, *85*, 535–547.

[11] M. Senger, S. Mebs, J. Duan, O. Shulenina, K. Laun, L. Kertess, F. Wittkamp, U.-P. Apfel, T. Happe, M. Winkler, M. Haumann, S. T. Stripp, *Phys. Chem. Chem. Phys.* **2018**, *20*, 3128–3140.

[12] M. Senger, K. Laun, F. Wittkamp, J. Duan, M. Haumann, T. Happe, M. Winkler, U.-P. Apfel, S. T. Stripp, *Angew. Chemie Int. Ed.* **2017**, *56*, 16503–16506.

[13] K. Laun, I. Baranova, J. Duan, L. Kertess, F. Wittkamp, U.-P. Apfel, T. Happe, M. Senger, S. T. Stripp, *Dalt. Trans.* **2021**, *50*, 3641–3650.